

“© 2020 IEEE. Personal use of this material is permitted. Permission from IEEE must be obtained for all other uses, in any current or future media, including reprinting/republishing this material for advertising or promotional purposes, creating new collective works, for resale or redistribution to servers or lists, or reuse of any copyrighted component of this work in other works.”

Accurate Channel Estimation for Frequency-Hopping Dual-Function Radar Communications

Kai Wu*, Y. Jay Guo*, Xiaojing Huang* and Robert W. Heath Jr.†

*Global Big Data Technologies Centre, University of Technology Sydney, Sydney, Australia

†Department of Electrical and Computer Engineering, University of Texas at Austin, Austin, USA

Email: {Kai.Wu; Jay.Guo; Xiaojing.Huang}@uts.edu.au; rheath@utexas.edu

Abstract—Dual-function radar communications (DFRC) is proposed recently to embed information into radar waveform, and hence performs data communications by sharing radar apertures and frequency resources. Exploiting a frequency-hopping (FH) MIMO radar, DFRC can achieve the symbol rate that is larger than the radar pulse frequency. However, this requires an accurate channel estimate, which is challenging to achieve due to the non-cooperative radar transmission and the fast-changing FH waveform. In this paper, we propose an accurate channel estimation method for the DFRC based on FH-MIMO radars. We design a new FH-MIMO radar waveform which incurs no change to the ranging performance of the radar. The new waveform also enables a communication receiver to estimate the channel without knowing the pairing between hopping frequencies and antennas. We also develop a new angle estimation method at a single-antenna communication receiver using as few as one symbol, i.e., a single hop. Simulations are provided to validate the efficacy of the proposed channel estimation method. Specifically, the symbol error rate achieved based on the estimated channel approaches to that based on the ideal channel.

Index Terms—DFRC, FH, MIMO, waveform, channel estimation, angle estimation

I. INTRODUCTION

There have been increasing demands for systems with both communications and radar sensing capabilities, on emerging platforms such as unmanned aerial vehicles and smart cars [1]–[3]. Instead of having two separate systems, it is possible to develop joint communications and radar sensing (JCAS) techniques to integrate the two functions into one by sharing hardware and signal processing modules, and achieve immediate benefits of reduced cost, size, weight, and better spectrum efficiency. Dual-function radar communications (DFRC) is such an integration which uses the same radar aperture and frequency resource to transmit communication data [4].

Information embedding into radar waveform is a critical issue in DFRC. On one hand, a high achievable rate is pursued for communications; but on the other hand, only little or no impact is expected on the primary radar detection. The two design goals generally contradict each other. Some researchers optimize the beam pattern of a MIMO radar to perform conventional modulations, such as phase shift keying (PSK) and amplitude shift keying (ASK), using sidelobes [5], [6].

Others optimize the MIMO radar waveform to carry out non-traditional modulations, such as waveform shuffling [7] and code shift keying (CSK) [8]. These works [5]–[8] generally embed one symbol per radar pulse and hence the symbol rate is limited by the pulse repetition frequency (PRF) [4].

Recently, the DFRC based on frequency-hopping (FH) based MIMO (FH-MIMO) radars has attracted extensive attention [9]–[15], since FH-MIMO radar is able to achieve the information embedding in fast-time sub-pulses within a pulse repetition interval (PRI). There are mainly two methods for information embedding in FH-MIMO radars. The first method modulates the phases of the radar signals in each hop to perform PSK [11]–[14]. To decode PSK symbols, a communication receiver needs an accurate estimate of the channel response. The second method exploits different combinations of hopping frequencies as constellation symbols, referred to as FH code selection (FHCS) [15], but does not require channel estimation. The achievable rate of FHCS is limited by the number of combinations of hopping frequencies. Nevertheless, the achievable rate of FHCS can be improved, e.g., by performing PSK simultaneously, given an accurate channel estimation (as will be illustrated in Section V).

Although an accurate channel estimate plays an important role in the FH-MIMO radar-based DFRC, how to estimate channel has not been addressed yet in the literature. Moreover, it can be challenging to estimate channel in DFRC due to the following reasons. *First*, training signals for channel estimation in DFRC can only be designed by modifying any given radar waveforms, which potentially leads to an undesirable performance trade-off between channel estimation and radar detection. *Second*, the pairing between hopping frequencies and antennas is required for channel estimation (as will be clear in Section II-C); however, how to acquire the pairing information at a communication receiver is non-trivial in practice. Moreover, the fast-changing FH-MIMO radar waveform requires a communication receiver to update the pairing information on a sub-pulse basis [11], [15].

This paper proposes an accurate method for channel estimation in the FH-MIMO radar-based DFRC by tackling the above challenges. We design a new FH-MIMO radar waveform, which on one hand incurs no change to the radar ranging performance, and on the other hand enables the communication receiver to estimate the channel without acquiring the pairing between hopping frequencies and antennas. We also propose a

This work was supported in part by the Australian Research Council under Grant DP160102219, in part by the UTS DVC-R Funding Initiative for Research Strengths, and in part by the FEIT Post Thesis Industrial Scholarship.

new angle estimation method which can produce an accurate angle estimation using as few as only a single symbol, i.e., a single hop. Simulations are provided to validate the efficacy of the proposed channel estimation method. Specifically, the symbol error rate achieved based on the estimated channel approaches to that achieved using the ideal channel.

II. SIGNAL MODEL AND PROBLEM FORMULATION

Consider a DFRC system based on a FH-MIMO radar which also performs downlink communications for a single-antenna user terminal. The transmitter and receiver of the radar are co-located uniform linear arrays with N_T and N_R antennas, respectively. Let $\mathbf{s}(t) \in \mathcal{C}^{N_T \times 1}$ denote the signal vector radiated out by the MIMO transmitter array at time t ; $\alpha_g(t)$ denote the target reflection coefficient; θ_g denote the target direction seen by the MIMO radar; and $\mathbf{a}(\theta_g)$ and $\mathbf{b}(\theta_g)$ denote the MIMO transmitter and receiver array steering vectors, respectively¹. Here, the variables with subscript $(\cdot)_g$ are associated with the g -th target. The signal vector received by the MIMO receiver array can be modeled as [12], [15]

$$\mathbf{x}(t) = \sum_{g=0}^{N_t-1} \alpha_g(t) \mathbf{a}^T(\theta_g) \mathbf{s}(t) \times \mathbf{b}(\theta_g) + \mathbf{n}(t), \quad (1)$$

where N_t is the total number of targets and $\mathbf{n}(t) \in \mathcal{C}^{N_R \times 1}$ is the vector of additive white Gaussian noise (AWGN) at the MIMO receiver antennas.

A. FH-MIMO Radar

The FH-MIMO radar has the centroid frequency of the transmitted signal hop multiple times per PRI. With reference to [15], we divide the frequency band of a MIMO radar evenly into N_{SB} sub-bands, each having the centroid frequency as $f_k = f_L + \frac{kB}{N_{SB}}$ ($k = 0, 1, \dots, N_{SB} - 1$), where f_L is the starting frequency of the system frequency band and B is the radar bandwidth. In the FH-MIMO radar, the centroid frequency of the h -th hop ($h = 0, 1, \dots, H - 1$) in the p -th PRI ($p = 0, 1, \dots, P - 1$) at antenna m , denoted by $f_{ph}^{(m)}$, can take $f_k \forall k$ with an equal probability, i.e.,

$$f_{ph}^{(m)} \sim \mathcal{U}_{\mathcal{F}}, \quad \mathcal{F} = \{f_k \forall k \in [0, N_{SB} - 1]\}, \quad (2)$$

where $\mathcal{U}_{\mathcal{F}}$ denotes the uniform distribution in \mathcal{F} .

Let $[\mathbf{s}(t_{ph})]_m$ denote the transmitted signal from antenna m in the h -th hop and p -th PRI, where

$$pT + \frac{hT}{H} \leq t_{ph} \leq pT + \frac{(h+1)T}{H}, \quad (3)$$

and T denotes the PRI. Exploiting sinusoidal signal as the FH-MIMO radar waveform in each hop, $[\mathbf{s}(t_{ph})]_m$ becomes

$$[\mathbf{s}(t_{ph})]_m = e^{j2\pi f_{ph}^{(m)} t_{ph}}. \quad (4)$$

To ensure the waveform orthogonality of a MIMO radar, it is required that the centroid frequencies across antennas are different at any hop, i.e., $f_{ph}^{(m)} \neq f_{ph}^{(m')}, \forall m \neq m', \forall h$ [16].

¹As the radar transmitter and receiver are co-located, they “see” the target from the same direction [15].

B. Information Embedding for Communications

As in the previous works [11]–[16], we consider the line-of-sight (LoS) communication between the FH-MIMO radar and a single-antenna communication receiver. Let ϕ denote the angle-of-departure (AoD) of the LoS path with respect to (w.r.t.) the radar transmitter array. The multiple-input-single-output (MISO) channel vector can be given by $\beta(t)\mathbf{a}(\phi)$ with $\beta(t)$ and $\mathbf{a}(\phi)$ denoting the path response and the steering vector, respectively. Accordingly, the signal received by the communication receiver is given by

$$y(t) = \beta(t)\mathbf{a}^T(\phi)\mathbf{s}(t) + \xi(t), \quad (5)$$

where $\xi(t)$ is a zero-mean AWGN at the communication receiver with the variance of σ_{ξ}^2 .

Two communication constellations, PSK [11]–[14] and FHCS [15], are available to embed information into $\mathbf{s}(t)$. They are briefly introduced below

a) PSK modulates the phase of $[\mathbf{s}(t_{ph})]_m$ to convey information bits for communications. Specifically, a phase term $\mathcal{F}_m(t_{ph}) = e^{j\omega_{ph}^{(m)}}$ is multiplied to $[\mathbf{s}(t_{ph})]_m$ at the radar transmitter. Here, $\omega_{ph}^{(m)}$ spans the following PSK constellation

$$\omega_{ph}^{(m)} \in \Omega_J = \left\{ 0, \frac{2\pi}{2^J}, \dots, \frac{2\pi(2^J - 1)}{2^J} \right\}, \quad (6)$$

where J denotes the information bits per hop. We see from (5) that the PSK phases are coupled with the phases of $\beta(t)$ and the elements of $\mathbf{a}(\phi)$ in a multiplicative manner. Therefore, to decode PSK symbols, we need the following information:

- 1) the pairing between hopping frequencies and radar transmitter antennas; and
- 2) the accurate estimations of $\beta(t)$ and ϕ to suppress the phase terms incurred by the channel.

b) FHCS exploits the combination of hopping frequencies to convey information bits. As seen from (2), we have N_{SB} available centroid frequencies and only $N_T (< N_{SB})$ frequencies are selected per hop. Thus, there are $C_{N_{SB}}^{N_T}$ different combinations of hopping frequencies in overall. In FHCS, each combination is regarded as a communication symbol. At the communication receiver, the FHCS symbol can be identified by only detecting the N_T hopping frequencies, which therefore does not require the pairing and channel information.

Nevertheless, we see from (5) that FHCS can be performed in combination with PSK to improve communication achievable rate. Since the hopping frequencies can be identified regardless of the initial phases of the received signals, FHCS symbols can be decoded unaffected by PSK modulations. With the hopping frequencies identified, the PSK decoding can be performed given an accurate channel estimate and the pairing between hopping frequencies and antennas.

C. Problem Formulation and Practical Challenges

From the above elaborations on PSK and FHCS, we see that an accurate channel estimation is important to FH-MIMO

radar-based DFRC systems. However, it is challenging to estimate the channel at a single-antenna communication receiver with a non-cooperative radar transmitter, as analyzed below.

Substituting (4) into (5) and after down-conversion (with the local oscillator frequency f_L) and digitization (with the sampling interval T_s), $y(t)$ at hop h and PRI p becomes

$$y(i) = \beta \sum_{m=0}^{N_T-1} e^{-j2\pi m d \frac{\sin \phi}{\lambda}} \times e^{-j2\pi \frac{k_{ph}^{(m)} B}{N_{SB}} iT_s} + \xi(i), \quad (7)$$

where $i(=0, 1, \dots, L-1)$ is the sample index; β is assumed fixed in the short period of t_{ph} , see (3); $e^{-j2\pi \frac{k_{ph}^{(m)} B}{N_{SB}} iT_s}$ is the m -th element of $\mathbf{a}(\phi)$; and $\frac{k_{ph}^{(m)} B}{N_{SB}} = f_{ph}^{(m)} - f_L$ is the baseband frequency. By taking the discrete Fourier transform (DFT) of $y(i)$, the frequency-domain received signal, denoted by $Y(l)$, can be calculated as in

$$\begin{aligned} Y(l) &= \sum_{i=0}^{L-1} y(i) e^{-j\frac{2\pi i l}{L}} \\ &= \beta \sum_{m=0}^{N_T-1} e^{-j2\pi m d \frac{\sin \phi}{\lambda}} \times \underbrace{\left[\sum_{i=0}^{L-1} e^{j2\pi \frac{k_{ph}^{(m)} B}{N_{SB}} iT_s} e^{-j\frac{2\pi i l}{L}} \right]}_{\mathcal{A}_{ph}^{(m)}(l)} \\ &\quad + \Xi(l), \end{aligned} \quad (8)$$

where $\Xi(l)$ is the DFT of $\xi(i)$.

According to (8), we can extract the signal from the m -th antenna by identifying the hopping frequency at antenna m , i.e., $k_{ph}^{(m)}$. However, this requires the pairing between hopping frequencies and antennas, which may not be available at the communication receiver. Moreover, FH-MIMO radar changes the hopping frequencies on the sub-pulse basis [15]. Such a fast updating of the pairing information at a communication receiver can be difficult in DFRC, if not impossible.

In communications, the specifically designed training signals are used for channel estimation and known between a pair of communication transmitter and receiver. Conversely, the training signals can only be designed by modifying radar waveform in DFRC. The waveform modification that is favorable for channel estimation can degrade the performance of the primary radar detection, leading to the performance trade-off between radar detection and channel estimation. To this end, the training signals need to be designed holistically with little or no impact incurred on the primary radar detection.

III. A NOVEL FH-MIMO WAVEFORM FOR CHANNEL ESTIMATION IN DFRC

In this section, we present a novel FH-MIMO radar waveform which is designed by re-ordering the hopping frequencies of the original FH-MIMO radar in an ascending order². The new waveform is given by

$$[\tilde{\mathbf{s}}(t_{ph})]_m = e^{j2\pi \tilde{f}_{ph}^{(m)} t_{ph}}, \quad \tilde{f}_{ph}^{(0)} < \tilde{f}_{ph}^{(1)} < \dots < \tilde{f}_{ph}^{(N_T-1)}, \quad (9)$$

²It can be in either ascending or descending order, which does not affect the channel estimation method to be proposed.

where the same group of hopping frequencies are used as those in the original radar, i.e., $\{\tilde{f}_{ph}^{(m)} \forall m\} = \{f_{ph}^{(m)} \forall m\}$. Note that the new waveform $[\tilde{\mathbf{s}}(t_{ph})]_m$ replaces the pairing between hopping frequencies and antennas with a deterministic ordering of the hopping frequencies.

A good property of the new waveform is that it does not incur any change to the ranging performance of the FH-MIMO radar, as dictated below.

Proposition 1: The new waveform $[\tilde{\mathbf{s}}(t_{ph})]_m$ has the same range ambiguity function as the original FH MIMO radar based on $[\mathbf{s}(t_{ph})]_m$ given in (4).

Proof: The proof is started by analyzing the range ambiguity function of an FH-MIMO radar. With reference to [17, Eq. (27)], the range ambiguity function, denoted by $|\chi(\tau)|$, can be expressed as

$$|\chi(\tau)| = \left| \sum_{m,m'=0}^{N_T-1} \sum_{h,h'=0}^{H-1} \underbrace{\kappa(\tilde{\tau}, \nu)}_{\mathcal{B}} e^{j2\pi \tilde{\nu} \frac{hT}{H}} \underbrace{e^{j2\pi f_{ph'}^{(m')} \tau}}_{\mathcal{D}} \right|, \quad (10)$$

where $\tilde{\tau} = \tau - \frac{T(h'-h)}{H}$, $\nu = f_{ph}^{(m)} - f_{ph'}^{(m')}$ and $\kappa(x, y)$ is the ambiguity function of a standard rectangular pulse. According to [17, Eq. (26)], we have $\kappa(x, y) = \left(\frac{T}{H} - |x|\right) \mathcal{S}\left(y\left(\frac{T}{H} - |x|\right)\right) e^{j\pi y(x + \frac{T}{H})}$, if $|x| < \frac{T}{H}$; and otherwise $\kappa(x, y) = 0$, where $\mathcal{S}(\alpha) = \frac{\sin(\pi\alpha)}{\pi\alpha}$ is a sinc function; and x and y span range and Doppler domains, respectively.

From (10), we see that any change of $f_{ph}^{(m)}$ in hop h has no impact on $f_{ph'}^{(m')}$ in hop h' , and vice versa. Thus, the set of combinations of $(\nu, f_{ph'}^{(m')})$ remain the same given any ordering of hopping frequencies in hops h and h' , since the combination is independent of element orderings [18]. We also see from (10) that the combinations, $(\mathcal{B}, \mathcal{D})$, are uniquely determined by the combinations of $(\nu, f_{ph'}^{(m')})$, since the other parameters, $\tilde{\tau}$ and τ , are independent of m or m' . Thus, we can conclude that the range ambiguity function, $|\chi(\tau)|$, remains the same given any ordering of hopping frequencies. ■

Fig. 1 plots the range ambiguity function of an FH-MIMO radar, where $N_T = 10$, $N_{SB} = 20$, $H = 15$, $B = 100$ MHz, and the hopping frequencies are randomly generated based on (2). The original waveform refers to the conventional FH-MIMO waveform without re-ordering which is widely used in the previous works [11]–[15]. We see that the ambiguity function using the new waveform overlaps with that using the original waveform, which is seen more obviously in the zoomed-in sub-figure. Thus, Proposition 1 is validated.

IV. PROPOSED CHANNEL ESTIMATION METHOD

We proceed to propose new algorithms to estimate the communication channel using the new FH-MIMO radar waveform. Seen from (7), the estimation of β can be readily obtained via a least square (LS) estimator. Therefore, we focus on the estimation ϕ in the following. For notation simplicity, we use $[\mathbf{s}(t_{ph})]_m$ given in (4) to denote the new waveform whose hopping frequencies, however, satisfies (9). Since the proposed

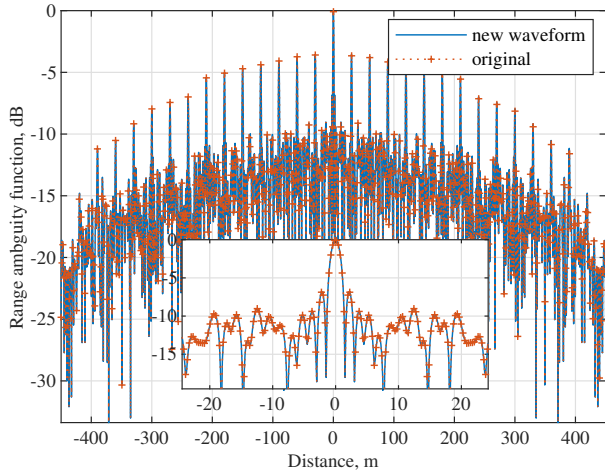


Fig. 1. Comparison of the range ambiguity function of a FH MIMO radar using the new and original waveforms, as given in (9) and (4), respectively.

method can work using a single hop, we focus on hop h in PRI p for illustration clarity. Extracting the received signal from the m -th antenna, we obtain

$$Y_m(l) = \beta e^{-j\frac{2\pi}{N_T}mu} \mathcal{A}_{ph}^{(m)}(l) + \Xi_m(l), \quad u = \frac{Md \sin \phi}{\lambda} \quad (11)$$

where $\mathcal{A}_{ph}^{(m)}(l)$ is the DFT enclosed in the square brackets in (8), and u is an auxiliary variable. Note that $\frac{2\pi u}{N_T}$ is a one-to-one mapping of $\phi \in [-\frac{\pi}{2}, \frac{\pi}{2}]$, since $|\frac{2\pi d \sin \phi}{\lambda}| \leq \pi$ always holds for $d \leq \frac{\lambda}{2}$.

To estimate u exploiting the signal $Y_m(l)$, we need to first suppress $\mathcal{A}_{ph}^{(m)}(l)$. By searching for the N_T largest peaks in $|Y(l)|$, the N_T hopping frequencies in hop h and PRI p can be identified and then used for calculating $\mathcal{A}_{ph}^{(m)}(l)$. Assume that $|Y(l)|$ takes peaks at $l_m^* \forall m$ which satisfies

$$0 \leq l_0^* < l_1^* < \dots < l_{N_T-1}^* \leq I - 1. \quad (12)$$

The new waveform ensures that the l_m^* -th peak corresponds to the signal radiated by the m -th antenna of the radar transmitter. By substituting (12) into (8), the hopping frequency of the m -th antenna can be identified as

$$\hat{k}_{ph}^{(m)} = \frac{N_{SB} l_m^*}{IBT_s}, \quad \hat{f}_{ph}^{(m)} = f_L + \frac{\hat{k}_{ph}^{(m)} B}{N_{SB}}. \quad (13)$$

According to (8), $\mathcal{A}_{ph}^{(m)}(l_m^*)$ can be calculated. Dividing both sides of (11) by $\mathcal{A}_{ph}^{(m)}(l_m^*)$ leads to

$$\tilde{Y}_m^* = \frac{Y_m(l_m^*)}{\mathcal{A}_{ph}^{(m)}(l_m^*)} = \beta e^{-j\frac{2\pi}{N_T}mu}, \quad m = 0, 1, \dots, N_T - 1, \quad (14)$$

where the noise term is omitted for now to illustrate the principle of the proposed method. The noise robustness of our new method will be shown in Section V.

We see from (14) that u can be regarded as a discrete frequency of a single-tone signal. By taking the DFT of \tilde{Y}_m^*

(over m), the integer part of u can be identified as the index of the peak of $|Z_{m'}|$, where $Z_{m'}$ is given by

$$Z_{m'} = \sum_{m=0}^{N_T-1} \tilde{Y}_m^* e^{-j\frac{2\pi m m'}{N_T}}, \quad m' = 0, 1, \dots, N_T - 1. \quad (15)$$

Let \tilde{m} denote the index of the peak. Using $\frac{2\pi \tilde{m}}{N_T}$ as the u estimate can lead to an estimation error up to the half of a frequency bin, i.e., $\frac{\pi}{N_T}$. To improve the estimation, interpolating DFT coefficients has been suggested in the literature [19]–[21]. Next, we develop the u estimation method based on the latest q -shift estimator (QSE), originally designed in [20] and improved in [21]. The proposed u estimation method is summarized in Algorithm 1.

Algorithm 1 Estimation of u

- 1: **Input** \tilde{Y}_m^* ($m = 0, 1, \dots, N_T - 1$), δ , ϵ .
- 2: Take the DFT of \tilde{Y}_m^* and obtain $Z_{m'}$, as shown in (15);
- 3: Identify the index of the peak of the DFT spectral $|Z_{m'}|^2$, denoted by \tilde{m} ;
- 4: Calculate the interpolated DFT coefficients, Z_{\pm} , see (17);
- 5: Construct γ as shown in (18);
- 6: Update δ and go back to Step 4 up to three times;
- 7: Calculate the final estimates of u and ϕ ; see (20).

In the input parameters of the algorithm, δ is an intermediate variable to be updated and $\delta = 0$ initially, and ϵ is a fractional interpolation factor, as given by [21, Eq. (23)]

$$\epsilon \leq \min\{N_T^{-\frac{1}{3}}, 0.32\}. \quad (16)$$

Step 2 calculates the DFT of \tilde{Y}_m^* followed by peak identification in Step 3. Note that the peak can be identified most reliably compared with any other spectral power responses, since the SNR of the peak is improved by as large as N_T times after the DFT [22].

In Step 4, the interpolated DFT coefficient Z_{\pm} is given by

$$Z_{\pm} = \sum_{m=0}^{N_T-1} \tilde{Y}_m^* e^{-j\frac{2\pi m(\tilde{m} + \delta \pm \epsilon)}{N_T}}, \quad (17)$$

which is in essence the DFT coefficient at the non-integer (i.e., $\tilde{m} + \delta \pm \epsilon$) frequency bin. In Step 5, γ is constructed by

$$\gamma = \frac{z_+ - z_-}{z_+ + z_-}, \quad (18)$$

which leads to an update of δ in Step 6 [20],

$$\delta = \frac{\epsilon \cos^2(\pi\epsilon)}{1 - \pi\epsilon \cot(\pi\epsilon)} \times \Re\{\gamma\} + \delta, \quad (19)$$

where δ in the right-hand side (RHS) of the equality is the old value, and $\Re\{\cdot\}$ takes the real part of a complex number. Note that the reason that we update δ up to three times is because the algorithm can generally converge after three iterations [20].

The final estimate of u can be given by $\hat{u} = \tilde{m} + \delta$, which, combined with (11), gives the estimate of ϕ , i.e.,

$$\hat{\phi} = \arcsin \frac{\hat{u}\lambda}{Md}, \quad \hat{u} = (\tilde{m} + \delta). \quad (20)$$

Substituting (20) into (14), we can estimate β as

$$\hat{\beta} = \frac{1}{N_T} \sum_{m=0}^{N_T-1} \tilde{Y}_m^* e^{j \frac{2\pi}{N_T} m \hat{u}}. \quad (21)$$

V. SIMULATION RESULTS

In this section, simulation results are provided to illustrate the performance of the proposed channel estimation method and its application in an FH-MIMO radar-based DFRC. Unless otherwise specified, the following parameters are used in the simulations: $f_c = 8$ GHz, $B = 100$ MHz, $K = 20$, $H = 10$, $T = 10 \mu\text{s}$, $N_T = 10$ and $\phi = 60^\circ$; and 2×10^4 independent runs are performed to obtain the averaged result in the figures.

Fig. 2 presents the estimation performance of the proposed Algorithm 1, where the CRLB of \hat{u} is $\frac{6}{2\pi^2 N_T \rho}$ with ρ denoting the estimation SNR [20]; and the CRLB of $\sin \hat{\phi}$ can be accordingly calculated based on (11). We see from Fig. 2 that the proposed u estimation can asymptotically approach the CRLB as the estimation SNR increases. This is consistent with [20], [21]. We also see that the estimation accuracy achieved by the proposed algorithm is very high. At the low SNR of -10 dB, the MSE of $\sin \hat{\phi}$ is only 10^{-3} ; and at the moderate SNR of 0 dB, the MSE reduces to below 10^{-5} .

Next, we demonstrate the impact of channel estimation on the communication performance of an FH-MIMO radar-based DFRC, where the modulations of BPSK [16] and FHCS [15] are simulated using the ideal and estimated channels. Note that PSK and FHCS can be combined for a higher achievable rate. Their combination, referred to as PFHCS, can be achieved with the new MIMO waveform and the accurate channel estimation. Specifically, the new waveform ensures the suppression of $\mathcal{A}_{ph}^{(m)}(l_m^*)$, as done in (14); and the obtained channel estimates can remove the impact of β and ϕ to enable the decoding of $\omega_{ph}^{(m)}$ given in (6). Furthermore, enabled by the accurate channel estimation, the combinations of hopping frequencies in FHCS can be replaced with the permutations of the frequencies. Therefore, we propose another transmission, referred to as FH permutation selection (FHPS). At the MIMO transmitter, FHPS pairs the hopping frequencies and antennas to convey different symbols of information bits. To detect the pairing at the communication receiver, we can substitute $\hat{\beta}$ and \hat{u} into (14) to estimate m .

Fig. 3 compares the achievable rates of different modulation schemes. We see that the proposed PFHCS and FHPS have much higher achievable rates than the benchmark schemes. The rate improvement achieved by PFHCS and FHPS can be as large as 10 Mbps and 21 Mbps, respectively, as compared to FHCS. Interestingly, we also see that PFHCS has a larger increasing rate than FHCS given large N_T which owes to the combination with BPSK. It is noteworthy that PFHCS and FHPS are enabled by the new MIMO radar waveform and the accurate channel estimation method.

Fig. 4 compares the symbol error rate (SER) of different transmission schemes, where the channel estimations in Fig. 2 are applied for decoding. Note that the bit energy to noise ratio (BENR), i.e., $\frac{E_b}{N_0}$, is considered in the x -axis. This provides

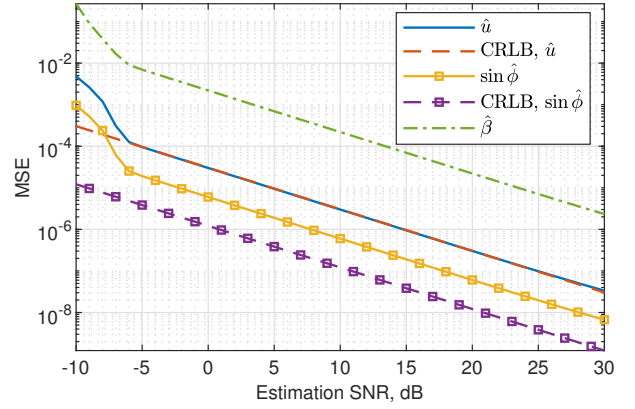


Fig. 2. MSE of channel estimates versus the estimation SNR.

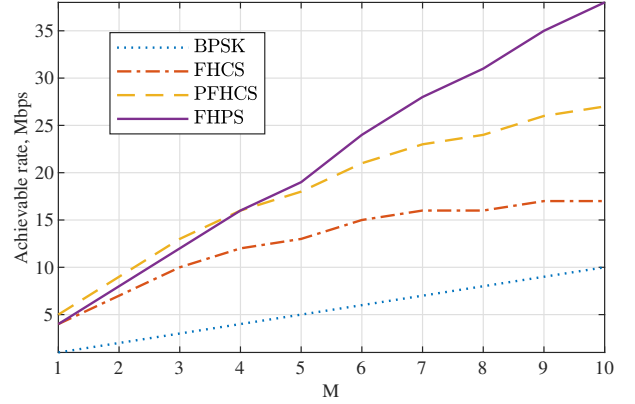


Fig. 3. Achievable rate versus antenna number, where BPSK [16] and FHCS [15] are benchmark transmissions; and PFHCS and FHPS are new transmission schemes enabled by the new MIMO waveform (9) and Algorithm 1.

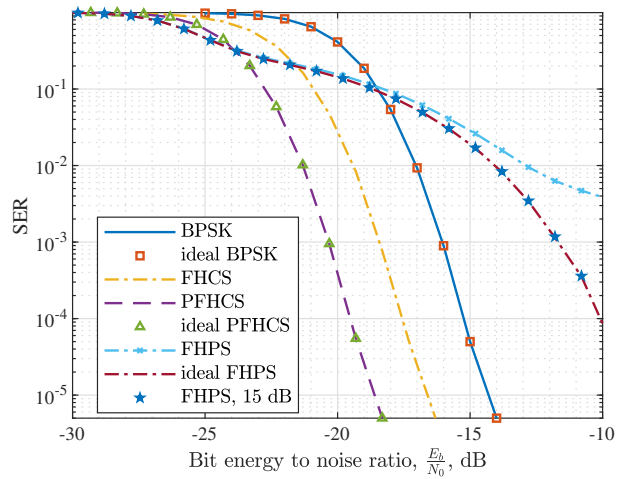


Fig. 4. SER versus BENR, where “ideal” in the legend indicates that the ideal channel information and the pairing information are used for the transmission; and the curve “FHPS 15dB” exploits the channel estimations obtain at $\rho = 15$ dB, and the other curves use the estimations at $\rho = 0$ dB.

a fair comparison between the different modulation schemes since they have drastically different number of bits per symbol

[15]. We see that using the proposed channel estimation method can produce the same SER as using the ideal channel, which validates the high accuracy of the proposed method. We also see that PFHCS achieves the best SER performance among the schemes owing to the proposed FH-MIMO waveform. We further see that FHPS is more prone to channel estimation errors compared with BPSK and PFHCS, and its SER performance becomes worse than the other schemes when BENR, i.e., $\frac{E_b}{N_0}$, becomes larger -19.5 dB. This is caused by the larger error probability of identifying an ordered set, as compared to a non-ordered one [18].

VI. CONCLUSION

This paper develops an accurate channel estimation method for the FH-MIMO radar-based DFRC. This is achieved by a new FH-MIMO radar waveform which does not incur any change to the ranging performance of the radar and enables the communication receiver to estimate channel without the pairing between hopping frequencies and antennas. This is also enabled by an accurate angle estimation method which uses as few as a single symbol. Simulation results show that the SER achieved based on the estimated channel approaches to that using the ideal channel.

REFERENCES

- [1] J. A. Zhang, X. Huang, Y. J. Guo, J. Yuan, and R. W. Heath, "Multibeam for joint communication and radar sensing using steerable analog antenna arrays," *IEEE Trans. Veh. Technol.*, vol. 68, no. 1, pp. 671–685, Jan 2019.
- [2] V. Petrov *et al.*, "On unified vehicular communications and radar sensing in millimeter-wave and low Terahertz bands," *IEEE Wireless Commun.*, vol. 26, no. 3, pp. 146–153, June 2019.
- [3] P. Kumari, S. A. Vorobyov, and R. W. Heath, "Adaptive virtual waveform design for millimeter-wave joint communication-radar," *IEEE Trans. Signal Process.*, pp. 1–1, 2019.
- [4] A. Hassanien, M. G. Amin, E. Aboutanios, and B. Himed, "Dual-function radar communication systems: A solution to the spectrum congestion problem," *IEEE Signal Process. Mag.*, vol. 36, no. 5, pp. 115–126, Sep. 2019.
- [5] A. Hassanien, M. G. Amin, Y. D. Zhang, and F. Ahmad, "Dual-function radar-communications: Information embedding using sidelobe control and waveform diversity," *IEEE Trans. Signal Process.*, vol. 64, no. 8, pp. 2168–2181, April 2016.
- [6] X. Wang, A. Hassanien, and M. G. Amin, "Dual-function MIMO radar communications system design via sparse array optimization," *IEEE Trans. Aerosp. Electron. Syst.*, vol. 55, no. 3, pp. 1213–1226, June 2019.
- [7] A. Hassanien, E. Aboutanios, M. G. Amin, and G. A. Fabrizio, "A dual-function MIMO radar-communication system via waveform permutation," *Digit. Signal Process.*, vol. 83, pp. 118–128, 2018.
- [8] T. W. Tedesso and R. Romero, "Code shift keying based joint radar and communications for EMCON applications," *Digit. Signal Process.*, vol. 80, pp. 48–56, 2018.
- [9] C. Yang, M. Wang, L. Zheng, and C. Tang, "Dual function system with shared spectrum using FMCW," *IEEE Access*, vol. 6, pp. 79 026–79 038, 2018.
- [10] S. Y. Nusenu, W.-Q. Wang, and H. Chen, "Dual-function MIMO radar-communications employing frequency-hopping chirp waveforms," *Progress In Electromagnetics Research*, vol. 64, pp. 135–146, 2018.
- [11] I. P. Eedara, A. Hassanien, M. G. Amin, and B. D. Rigling, "Ambiguity function analysis for dual-function radar communications using PSK signaling," in *2018 52nd Asilomar Conf. on Signals, Syst., and Computers*, Oct 2018, pp. 900–904.
- [12] I. P. Eedara and M. G. Amin, "Dual function FH MIMO radar system with DPSK signal embedding," in *2019 27th European Signal Process. Conf. (EUSIPCO)*, Sep. 2019, pp. 1–5.
- [13] I. P. Eedara and M. G. Amin, "Performance trade-off analysis of co-design of radar and phase modulated communication signals in frequency hopping MIMO systems," in *Big Data: Learning, Analytics, and Applications*, vol. 10989. Intern. Society for Optics and Photonics, 2019, p. 109890K.
- [14] I. P. Eedara, M. G. Amin, and A. Hassanien, "Analysis of communication symbol embedding in FH MIMO radar platforms," in *2019 IEEE Radar Conf. (RadarConf)*, April 2019, pp. 1–6.
- [15] W. Baxter, E. Aboutanios, and A. Hassanien, "Dual-function MIMO radar-communications via frequency-hopping code selection," in *2018 52nd Asilomar Conf. on Signals, Syst., and Computers*, Oct 2018, pp. 1126–1130.
- [16] X. Wang and J. Xu, "Co-design of joint radar and communications systems utilizing frequency hopping code diversity," in *2019 IEEE Radar Conf. (RadarConf)*, April 2019, pp. 1–6.
- [17] C. Chen and P. P. Vaidyanathan, "MIMO radar ambiguity properties and optimization using frequency-hopping waveforms," *IEEE Trans. Signal Process.*, vol. 56, no. 12, pp. 5926–5936, Dec 2008.
- [18] K. P. Bogart, *Introductory combinatorics*. Academic Press, Inc., 2004, ch. 2.3 Combinations (subsets) of sets.
- [19] E. Aboutanios and B. Mulgrew, "Iterative frequency estimation by interpolation on Fourier coefficients," *IEEE Trans. Signal Process.*, vol. 53, no. 4, pp. 1237–1242, April 2005.
- [20] A. Serbes, "Fast and efficient sinusoidal frequency estimation by using the DFT coefficients," *IEEE Trans. Commun.*, vol. 67, no. 3, pp. 2333–2342, March 2019.
- [21] K. Wu, W. Ni, J. A. Zhang, R. P. Liu, and Y. J. Guo, "Refinement of optimal interpolation factor for DFT interpolated frequency estimator," *IEEE Commun. Lett.*, pp. 1–1, 2020.
- [22] K. Wu, W. Ni, T. Su, R. P. Liu, and Y. J. Guo, "Robust unambiguous estimation of angle-of-arrival in hybrid array with localized analog subarrays," *IEEE Trans. Wireless Commun.*, vol. 17, no. 5, pp. 2987–3002, May 2018.